Energy Transfer Studies of Interpenetrating Polymer Networks: Characterizing the Interface in Polyacrylate−Polyurethane IPNs

Yahya Rharbi, Ahmad Yekta, and Mitchell A. Winnik*

Department of Chemistry, University of Toronto, 80 St. George Street Toronto, Ontario, Canada M5S 3H6

Robert J. DeVoe and Denise Barrera

3M Corporate Research Laboratories, St. Paul, Minnesota 55144-1000

Received October 6, 1998; Revised Manuscript Received March 8, 1999

ABSTRACT: Interpenetrating polymer networks (IPNs) of polyurethane (PU) and polyacrylate (PA) were prepared to give very small domains (ca. 20 nm) of PA dispersed in a PU matrix. In these samples the PU phase is labeled with phenanthrene, a donor for energy transfer experiments, and the PA phase is labeled with anthracene, the corresponding acceptor. Direct nonradiative energy transfer from phenanthrene to anthracene was used to study the IPN morphology. The interface and mixing between the microphases were analyzed in terms of a Helfand and Tagami (H−T) profile, which is commonly used to describe the interface in polymer blend systems. Exact fluorescence theoretical decay profiles were calculated according to the H−T profiles in a restricted geometry. Experimental fluorescence decays were compared to the theoretical decays, and the interface thickness was recovered. At the level of the model we used in our analysis, we found strong similarities between these IPNs and traditional polymer blends.

Introduction

Interpenetrating networks (IPNs) are an important class of materials with broad interest from both fundamental[1−3] and industrial[4,5] points of view. These IPNs are normally made up of two or more incompatible cross-linked polymers in which the cross-linking is used to increase the extent of mixing of the networks. Various theoretical and experimental studies have focused on the relationship between the extent of mixing and the corresponding network properties. De Gennes predicted that spatial fluctuations of the microphases occur as a consequence of polymer immiscibility and network cross-linking.[6] In practice, the final structure of many IPNs is found to be strongly affected by the kinetics of polymerization and the timing of phase separation.

Urethane−acrylate IPNs represent a particularly interesting system because the two components can be cured independently, which facilitates morphology control.[7−9] In these IPNs, the rate of urethane polymerization can be controlled by the temperature and the amount of catalyst. The rate of acrylate polymerization can be controlled by photochemical initiation. In a previous report from our laboratory, Yang and Winnik[10] demonstrated that the morphology of these urethane-rich IPNs is a sensitive function of the processing parameters. Polymerization of the acrylate prior to the urethane leads to a structure with large acrylate domains (>2000 nm). In contrast, polymerization of the urethane prior to the acrylate leads to small acrylate domains (20 nm). In the present report, we focus on the study of the morphology of very similar IPNs consisting of small acrylate domains in a urethane matrix.

IPNs are a subgroup of the broad class of polymer blends.[1,11] The extent of mixing in IPNs, and in polymer blends in general, is characterized by two major parameters: domain size, which is related to the total surface of contact between the two polymers, and the extent of interfacial mixing. In the simple case of polymer blends (without cross-linking), the extent of interfacial mixing is determined by the magnitude of the polymer interaction, as described by the Flory−Huggins parameter χ. Helfand and Tagami used a mean field theory to predict the mixing profiles of blends.[12] Various research groups have carried out experiments designed to characterize interfacial mixing in polymer blends.[13,14] It is well-established that cross-linking of polymers affects the domain size of blends,[1] but it is not clear whether cross-linking also affects interfacial mixing. Transmission election microscopy (TEM) and scattering techniques are the most common methods used to characterize the domain size in blends and in IPNs. The extent of interfacial mixing is more difficult to study, and the most common methods involve NMR and scattering experiments.[15] Brulet et al.[15a] have examined the extent of interfacial mixing in several IPNs by small-angle neutron scattering (SANS). They found Porod law behavior in cases of IPNs with extended phase separation (large domains), which indicates a sharp interface relative to the domain size. For other cases, they found deviations from the Porod law, which might indicate fluctuations of the interface over distances comparable to the domain size.

Direct nonradiative energy transfer (DET)[16,17] has been used as a technique for interface characterization in cases of simple systems such as latex blends[13a] and block copolymers.[13b,c] Here we attempt to use the DET technique to study the interface between urethane and acrylate networks in a series of IPNs. In these experiments, the donor dye, phenanthrene, is incorporated into the urethane phase, and the acceptor dye, anthracene (An), is incorporated into the acrylate phase. We use a phenanthrene−diol derivative **1** to incorporate the donor into the urethane phase and an anthracene−diacrylate derivative **2** to incorporate the acceptor into the acrylate phase. The extent of energy transfer is a measure of the extent of mixing between the different phases. In contrast to latex blends and block copolymers, IPNs are complicated because of polydispersity of

10.1021/ma9815612 CCC: $18.00
Published on Web 04/28/1999

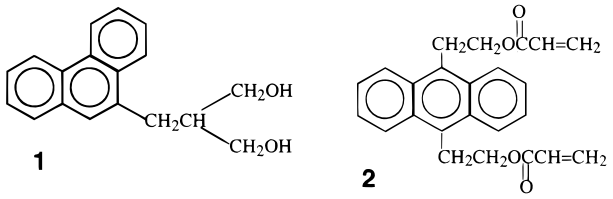

domain size and shape. To proceed with the analysis and to learn about the extent of interfacial mixing, we simplify our structure by considering spherical phase domains. Interfacial mixing in IPNs will be described by Helfand−Tagami profiles, commonly employed for interface characterization of simple polymer blends at equilibrium.

The study of DET in small domains (20 nm) requires the use of a proper theory of energy transfer. Here we use the theory of DET in restricted geometry developed by Klafter−Blumen[18] and generalized by Yekta et al.[19,20] to fit our experimental data.

Experimental Section

Materials. All IPN samples consist of 70% polyurethane and 30% polyacrylate. The polyacrylate was prepared from 10% diacrylate and 90% monoacrylate (Figure 1). The urethane was prepared from polytetramethylene glycol (**3**; 9 g; M_n = 1000; Dupont) and of tri-isocyanate (**4**; 3 g; Desmurdo N100, Miles Chem. Co.). The polyacrylate was prepared from 2-ethylhexyl acrylate (**6**; 5.4 g; Fluka) and 1,6-hexanediol diacrylate (**5**; 0.6 g cross-linker; Aldrich). The acrylate polymerization was initiated by using a photoinitiator (**7**; 15 mg; 2,2-dimethoxy-2-phenyl acetophenone; Aldrich). The urethane phase is labeled with 3-(9-phenanthryl)-2-hydroxymethyl propanol (**1**; 15 mg) prepared as described previously.[21] The acrylate phase is labeled with varying amounts of 9,10-bis(2′-ethyl)anthracene diacrylate **2**.

Synthesis of 9,10-Bis(2′-ethyl)anthracene Diacrylate. Anthracene-9,10-bis(2′-hydroxyethyl)anthracene (1.0 g, 3.76 mmol) prepared as described by Evans and Upton[21] was dried in a desiccator overnight and then suspended in 100 mL of dichloroethane at 5 °C under nitrogen. Freshly distilled acryloyl chloride (3.00 mL, 2.98 mmol) was added, followed by triethylamine (5.24 mL, 71 mmol). The mixture was stirred and allowed to warm to room temperature over 2 h. The reaction was then quenched by adding ice-cold water. The organic layer was separated, and the aqueous layer was extracted with 3 × 20 mL dichloroethane. The combined organic layer was washed with NaCl, dried over Na_2SO_4 and evaporated to yield an oily product. The pure product (**2**; 0.36 g) was obtained by chromatography on silica gel (1:4 ethyl acetate/hexane), mp 125−7 °C. Note that partial polymerization of the product may occur during the reaction and workup, and the yield may increase if a radical chain inhibitor is used during the reaction. ^{1}H NMR ($CDCl_3$, 200 MHz); δ 8.42 (4H, dd, J = 7.0, 3.6 Hz, An-H), 7.59 (4H, dd, J = 7.0, 3.6 Hz, An-H), 6.42 (2H, dd, J = 1.6, 17.6 Hz, =C−H), 6.15 (2H, dd, J = 10.0, 17.6 Hz, =C−H), 5.85 (2H, dd, J = 1.6, 10.0 Hz, =C−H), 4.57 (4H, t, J = 7.5 Hz, CH_2), 4.02 (4H, t, J = 7.5 Hz, CH_2). MS (EI) *m*/*e* (rel intensity): 374 (56, M^+), 302 (28), 230 (100), 217 (78), 202 (59), 189 (12). Mass Calcd for $C_{24}H_{22}O_4$: 374.1518. Found: 374.1503.

Sample Preparation. Phenanthrene−diol (**1**, 15 mg) was dissolved in the polymer diol (**3**, 9 g) at 50 °C over 20 min. The photoinitiator (**7**, 15 mg) was dissolved in the mixture of monoacrylate and diacrylate (6 g). This solution was then divided into two parts. Into the first part (Acr1, 2.7 g), An−diacrylate (**2**, 30 mg) was dissolved by heating the mixture to 50 °C for 20 min with magnetic stirring. The remaining 2.3 g is referred to as Acr2. Tri-isocyanate was added to both portions: 1.35 g to Acr1−An and 1.12 g to Acr2. Finally, six new solutions were prepared by mixing the three solutions prepared above, polymer−diol/Phe−diol, Acr1−An, and Acr2

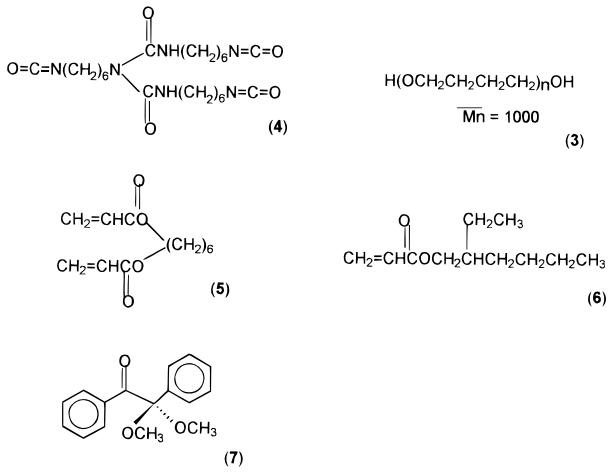

Figure 1. Structure of the monomers and the photoinitiator for IPN preparation.

Table 1

sample	polymer-diol, wt %	Acr1-An, wt %	Acr2, wt %	[phe], mM	[An], mM
IPN0	50	0	50	1.2	0
IPN1	50	7.59	42.4	1.2	2.38
IPN2	50	14.22	35.78	1.2	4.45
IPN3	50	23.8	26.2	1.2	7.45
IPN4	50	34.58	15.42	1.2	10.83
IPN5	50	50	0	1.2	15.6

(see Table 1), to make solutions with same amount of phenanthrene and varying concentrations of anthracene. To each of the six solutions, the catalyst (10 μL of a solution of a 2 wt % dibutyl dilaurate in ethyl acetate) was added via a 50 microliter syringe, and the solutions were shaken vigorously. The viscous solutions were then cast onto quartz plates (2 cm × 1 cm × 1 mm). The films (0.2−0.5 mm thick) were left in the dark at room temperature for 12 h. IR absorption at 2270 cm^{-1} was used to monitor the urethane polymerization, which went to completion in less than 12 h. Fluorescence decay measurements were then made on each of the IPN*i* (*i* = 0 to 5) samples. Next, the films were placed under nitrogen for 1 h and, finally, in the UV reactor to polymerize the acrylate. A Rayonet reactor equipped with RPR 3000 Å lamps combined with a KV-335 filter was used in photopolymerization of the acrylate. The KV-335 filter absorbs all light below 310 nm and protects the phenanthrene from photodecomposition in the presence of high-intensity UV light. The rate of polymerization was slower in the presence of An−diacrylate. The irradiation time of 15 min was chosen as that needed for the complete polymerization of the slowest reacting sample, IPN5. The IR absorption at 810 cm^{-1} was used to monitor the acrylate polymerization. The films, after irradiation, are referred to as IPN*i*−U (*i* = 0 to 5).

Another set of IPN samples was prepared using the procedure described above. Here the total fraction of acrylate/urethane was fixed (30/70 wt/wt, acrylate/urethane) and the amount of diacrylate in the monoacrylate was varied from 0 to 12 wt %. These samples were labeled with constant concentrations of phenanthrene and anthracene ([Phe] = 1.12 and [An] = 10 mM).

Fluorescence Decay Measurements. Fluorescence decay profiles were measured by the single-photon-timing technique.[16] The samples were excited at λ_{ex} = 300 nm, and phenanthrene fluorescence was detected at λ_{em} = 366 nm.[25] All decays were collected by taking 2 ×10^4 counts at the maximum intensity. Data were analyzed according to the Förster[22] and the Perrin models.[23] In this report, we also employ a more sophisticated method of data analysis. We approximate the IPN topology as being composed of spherical acrylate domains surrounded by a shell of urethane. The two

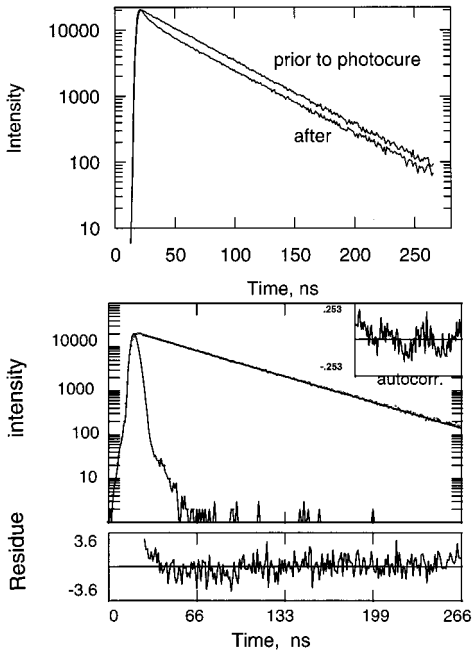

Figure 2. (a) Fluorescence decay of sample IPN0 (upper curve) prior to irradiation and (lower curve) after direct irradiation by RPR 3000 Å lamps of the Rayonet reactor. (b).Fluorescence decay of an identical sample, IPN0−U, after irradiation through a KV-335 filter. Here, the decay can be fitted by an exponential function ($\tau = 48.9$ ns with $\chi^2 = 1.13$).

phases are treated as though they interpenetrate according to a Helfand and Tagami profile.

Results and Discussion

Photopolymerization. We use fluorescence energy transfer from phenanthrene to anthracene as a tool to characterize the mixing of urethane and acrylate phases. Sample preparation presents many experimental difficulties. A prerequisite of good quality data from the DET analysis is that samples without acceptors (anthracene) should show a single-exponential decay of the emission of the donor (phenanthrene). The first problem we faced appeared during the photocure of the acrylate with the RPR 3000 Å lamps as the light source. We found nonexponential decays of phenanthrene, even in samples free of anthracene (Figure 2a). We note that the maximum intensity of the light source (300 nm) coincides with the maximum of phenanthrene absorption. We discovered that depending on the sample and its exposure time to the light source, some phenanthrene molecules photodecompose to give an unwanted signal. To avoid this problem, a KV-335 filter was used to protect phenanthrene from absorbing light.

A second problem encountered is one of quenching of phenanthrene by the photoinitiator of the acrylate polymerization.[10] In previous work, phenanthrene and the photoinitiator were found to act as a donor−acceptor pair for DET with a capture radius of $R_0 = 1$ nm. To minimize DET to aryl ketones groups formed by the photoinitiator, the amount of photoinitiator was reduced to 0.083 wt %. Under these conditions, we could obtain good exponential decays in samples free of anthracene. Under such conditions, the acrylate polymerization is slow. We also found that excess anthracene slows down the acrylate photocure rate through competitive light absorption. Therefore, the anthracene concentration used in the DET experiment was limited to 15 mM in order to complete the acrylate photocure in a reasonable

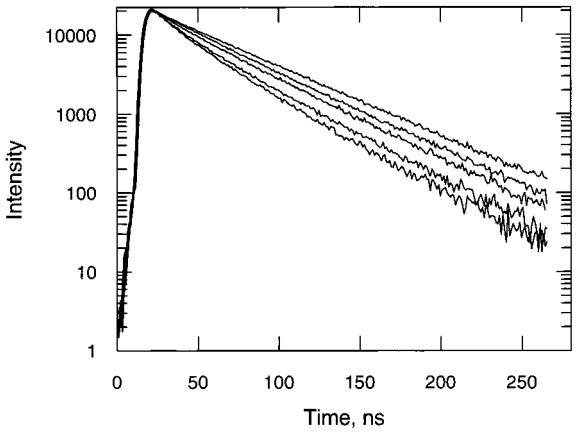

Figure 3. Fluorescence decays of samples IPN*i* before irradiation. From top to bottom, the anthracene concentrations in the film are 0, 2.38, 4.45, 7.45, and 10.83 mM.

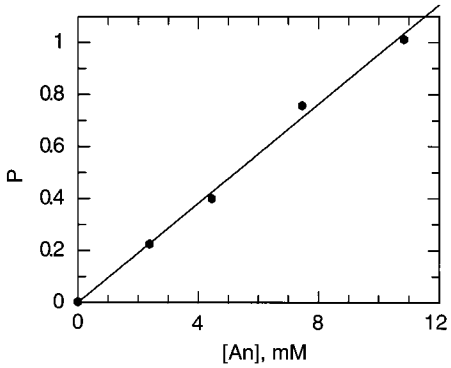

Figure 4. Anthracene-concentration dependence of the recovered value of P from the fit of the $I_D(t)$ profiles to the Förster model (eq 1).

time. We also investigated the possibility of anthracene photodecomposition and found this not to be a problem. Anthracene concentration was monitored by its UV absorption (400 nm) and was found not to change during the time of the acrylate photocure.

The phenanthrene decay of the anthracene-free sample before photocure (IPN0) fits well with a single-exponential expression ($\tau = 48.12$ ns and $\chi^2 = 1.09$). In the case where no precautions are taken in the photolysis process, the decay becomes nonexponential (Figure 2a) and is characterized by a fast lifetime (<10 ns), in addition to the unquenched phenanthrene lifetime (49 ns). The same sample, photocured under optimal conditions, shows a decay that fits a single-exponential profile (Figure 2b, $\tau = 48.9$ ns, and $\chi^2 = 1.13$). This is an important result, because it allows us to fit fluorescence decay data to sophisticated models in which all deviations from an exponential profile can be attributed to energy transfer.

Fluorescence Decays of IPN*i* (before photocure). The decays of the IPN*i* decrease faster as the An concentration increases (Figure 3). The data can be fitted to the Förster model[22] (eq 1) with χ^2 in the range 1−1.2 (Figure 4). By assuming rapidly reorienting chromophores, the Förster radius R_0 calculated from the slope of the plot of P versus [An] is 2.68 nm.

$$I_D(t) = I_o \exp(-t/\tau - P\sqrt{t/\tau})$$

$$P = \frac{4\pi^{3/2} N_A}{3000} R_o^3 [An] \qquad (1)$$

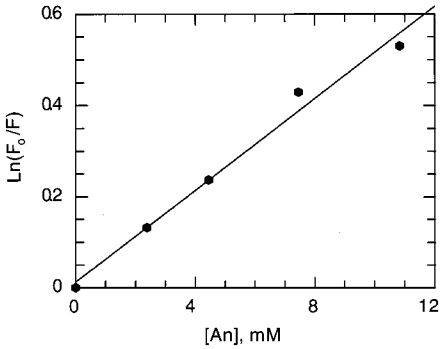

Figure 5. Anthracene concentration versus ln(F_0/F) for the fit of the $I_D(t)$ decays to the Perrin model (eq 2).

These data also can be fitted to the Perrin model[23]

$$\ln(F_o/F) = V_Q[\mathrm{An}]$$

$$V_Q = \frac{4\pi R_p^{\,3}}{3} \qquad (2)$$

where F and F_o are the time-integrated fluorescence intensities. These values are obtained from the normalized areas under the decay curves in the samples with anthracene (F) and in the anthracene-free sample (F_o). The individual decays were fitted with a sum of two exponential terms, and the normalized area (F) under the decay curve was calculated from this fit. Figure 5 shows a linear dependence of ln(F_o/F) upon the anthracene concentration. The Perrin radius R_p calculated from Figure 5 was found to be 2.7 nm. Both models assume that the samples have a random and frozen distribution of the phenanthrene and anthracene. Yang et al. in our laboratory[24] found a similar value of R_o = 2.67 nm in a urethane network covalently labeled with phenanthrene−diol and anthracene−diol.

At this stage in the process of the film preparation, the An−acrylate is free and phenanthrene is attached to the urethane polymer backbone. The films are swollen with the 30 wt % of free acrylate. Our results are consistent with the An−acrylate and the acrylate (solvent) being frozen on the nanosecond time scale. This point, however, needs further investigation.

Fluorescence Decays after Curing the Acrylate (IPN*i*−U). After polymerization of the acrylate inside the urethane network, polyacrylate demixes from the polyurethane and undergoes microphase separation. In previous experiments, microphase separation was observed by TEM[9b] (Figure 6). One can observe the effect of microphase separation by its effect on the phenanthrene fluorescence decays before and after photocure (Figure 7). After photocure, the decay is slower, from which we deduce that the amount of energy transfer from phenanthrene to anthracene is reduced. However the decays of the IPN*i*−U samples still decrease faster than the decay of the anthracene-free sample (see Figure 8). After phase separation, energy transfer still occurs in regions where the two polymers coexist, within the mixed region, or across a nearby interface. Note that for the small domains (ca. 20 nm) formed under these reaction conditions, energy transfer across the interface, from one phase to another, can occur with relatively high efficiency.[13]

The calculation of the mixing fraction between acrylate and urethane components can be evaluated by considering the difference of decay profiles before and after photocure. Areas under decays (F) (Figure 9) were calculated and normalized relative to those of samples with no anthracene. Considering the area under decays equivalent to the total fluorescence intensity, the efficiency of energy transfer ϕ_{ET} is calculated according to eq 3. Figure 10a shows the anthracene-concentration dependence of ϕ_{ET} before and after photocure. ϕ_{ET} is always lower after photocure, which is consistent with phase separation of the urethane and acrylate components. However, the result also indicates some degree of urethane and acrylate miscibility after photocure. The ratio of the ϕ_{ET} after and before photocure ($\Phi_{ET}^{after}/\Phi_{ET}^{prior}$) is related to the fraction of the quenched phenanthrene in the mixed region, and consequently, is related to the extent of mixing between urethane and acrylate. Figure 10b shows that this ratio is nearly independent of the anthracene concentration, and has

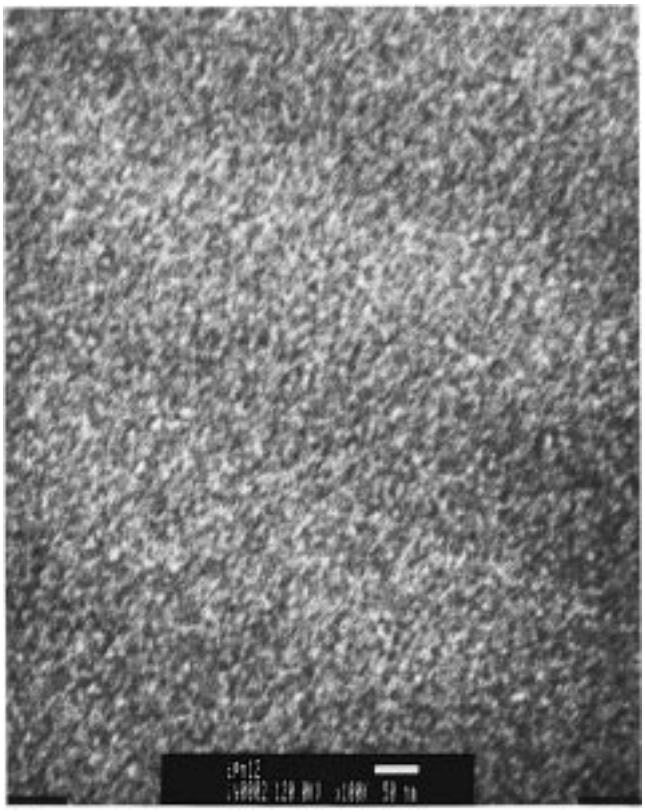

Figure 6. TEM image of an IPN made of 70% urethane and 30% acrylate, where polyurethane was cured prior to the polyacrylate. The urethane phase is stained selectively with RuO_4. Marker bar is 50 nm.

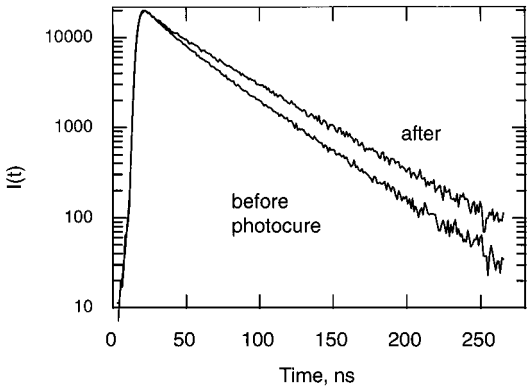

Figure 7. Fluorescence decays of sample IPN3 before (bottom curve) and after (top curve) photocure.

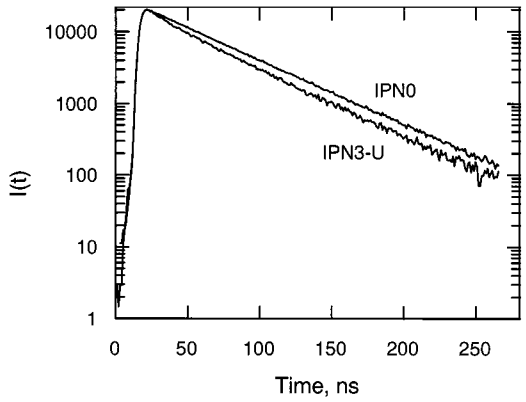

Figure 8. Fluorescence decay of sample IPN3−U after photocure (bottom curve) compared to that of the anthracene-free sample IPN0 (top curve).

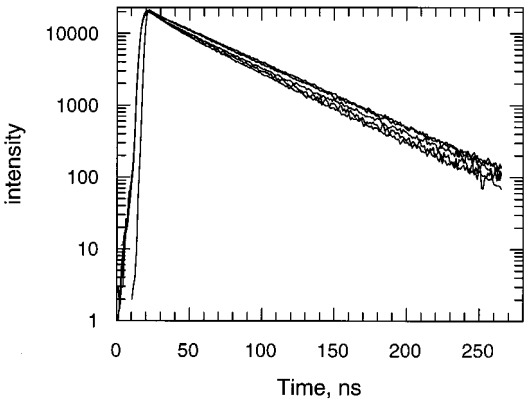

Figure 9. Fluorescence decays of the various IPNi−U samples after photocure. From top to bottom, the anthracene concentrations in the film are 0, 2.38, 4.45, 7.45, and 10.83 mM.

an average value of 0.4, which implies that 40% of the phenanthrene groups in the urethane are close enough to anthracene groups in the acrylate to undergo DET. This mixing between urethane and acrylate is of two kinds: (1) a high surface area of contact between these phases or (2) interfacial mixing (polymer−polymer interpenetration). In the following analysis, we try to quantify the contribution of each of these two effects to the observed energy transfer.

$$\phi_{ET} = 1 - \frac{F}{F_o} \tag{3}$$

Modeling the IPN System. De Gennes has predicted spatial fluctuations in IPN systems due to two opposing factors: immiscibility of the two polymers on one hand and polymer cross-linking on the other. Immiscibility of the polymers tends to create extended phase separation, but cross-linking tends to limit it. However, this theory does not predict the extent of interfacial mixing between the two phases nor their profiles. The spatial fluctuation in our IPN system (as observed by TEM)[9] is characterized by a mean distance of ca. 20 nm.

IPNs may be considered as a special case of polymer blends[1,11] where cross-linking limits the extent of phase separation. In recent years, polymer blend systems have been widely studied theoretically and experimentally. It is not clear how polymer cross-linking affects the density profile predicted for blends, and we can ask whether interfacial mixing in IPNs is controlled by the

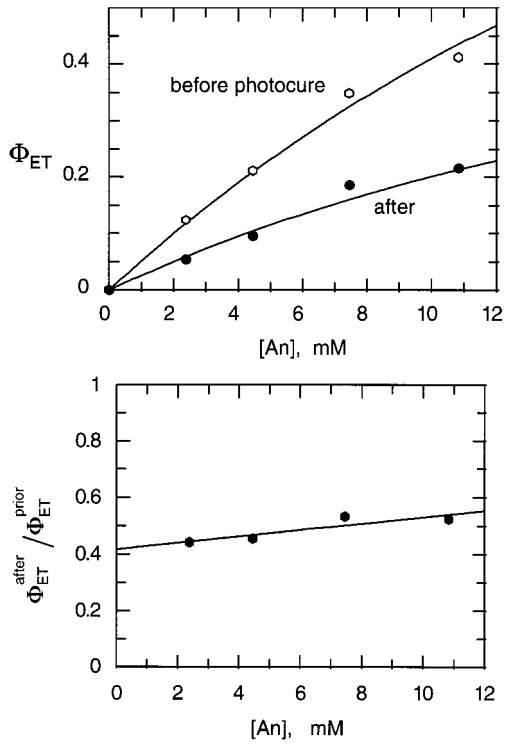

Figure 10. (a) Efficiency of energy transfer Φ_{ET} vs anthracene concentration for the samples before (top curve) and after photocure (bottom curve). (b) Anthracene-concentration dependence of the ratio of Φ_{ET} after and before photocure ($\Phi_{ET}^{after}/\Phi_{ET}^{prior}$).

polymer immiscibility or by cross-linking. In our present modeling of IPNs, we analyze the extent of interfacial mixing by assuming that the concentration profiles have the same shape as those predicted for polymer blends at equilibrium.

Variation of the Cross-linking Density. To contrast better the differences between blends and IPNs, we have studied IPNs in which the cross-linking density of the polyacrylate network was varied. A new set of samples was prepared, in which the fraction of total acrylate/urethane ratio was kept constant (acrylate/urethane $^{30}/_{70}$ wt/wt), but the amount of diacrylate cross-linker was varied from 0 to 12 wt. %. The concentrations of phenanthrene and anthracene were kept constant ([Phe] = 1.2 and [An] = 10 mM). These samples were prepared by the same procedure described in the Experimental Section: the urethane was completely cured over 48 h at room temperature (22 °C), and then the acrylate was photocured over 15 min.

The efficiency of energy transfer ϕ_{ET} calculated from the fluorescence decays of this set of samples do not show a significant dependence on the diacrylate concentration for the concentration range studied here (Figure 11). This result indicates that cross-linking of the polyacrylate network does not affect either the spatial fluctuations or the extent of mixing between the two phases. The semi-IPN (uncross-linked acrylate) is an interesting case, because it can be considered as the bridge between the IPN and a simple polymer blend. This semi-IPN might behave more like an ordinary polymer blend, because the polyacrylate is free to take any conformation inside the urethane network. Our results are consistent with the idea that the extent of interfacial mixing is controlled by polymer immiscibility and not by the extent of polymer cross-linking. In this

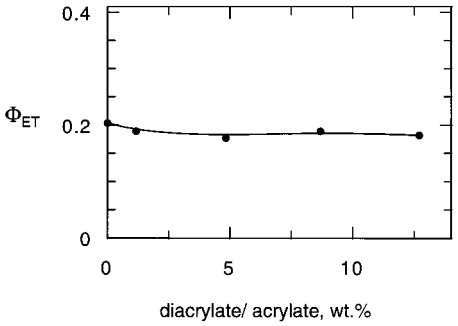

Figure 11. Efficiency of energy transfer plotted vs the diacrylate/acrylate ratio in the IPN formulation. The fraction of total acrylate to urethane and the concentrations of phenanthrene and anthracene were kept constant.

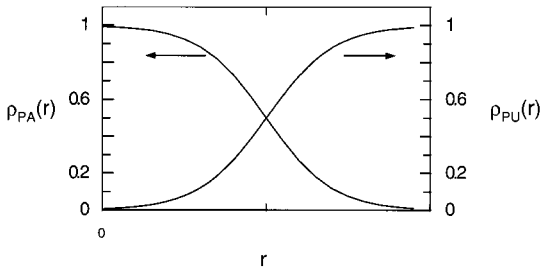

Figure 12. Representative plot of calculated Helfand−Tagami profiles for a urethane−acrylate blend. Here $\rho_{PU}(r)$ describes the distance dependence of the urethane segment density and $\rho_{PA}(r)$ describes the acrylate segment density. The fraction of urethane in the pure urethane phase is 1, and the fraction in the pure acrylate phase is 0.

way, we have some rationale for the analysis of the extent of interfacial mixing in our IPNs using the segment density profiles commonly used to characterize equilibrium polymer blends. (Figure 11).

Density Profiles. Miscibility in blends is dominated by the thermodynamics of the polymer−polymer interaction as characterized by the Flory−Huggins parameter χ. The density profiles ρ_{PU} and ρ_{PA} as predicted by Helfand and Tagami (H−T)[12] take the form

$$\rho_{PU}(r) = \left(\frac{1 + \tanh(2r/\delta)}{2}\right)$$

$$\rho_{PA}(r) = \left(\frac{1 - \tanh(2r/\delta)}{2}\right)$$

$$\delta = 2b/(6\chi)^{1/2} \qquad (4a)$$

where δ is the interface thickness (Figure 12) and b is the statistical monomer length. In the analysis below, we arbitrary assume that $b = 6-7$ Å. The concentration profiles of donor phenanthrene $C_D(r)$ and acceptor anthracene $C_A(r)$ are taken to be proportional to the segment densities of urethane and acrylate respectively, across the interface (eq 4),

$$C_D(r) = C_D^o \rho_{PU}(r)$$

$$C_A(r) = C_A^o \rho_{PA}(r) \qquad (4b)$$

where C_D^o and C_A^o are the molar concentrations of donor and acceptor in the pure urethane and acrylate phases. C_D^o and C_A^o are proportional to the known concentrations of phenanthrene and anthracene (C_D^o = [Phe]/0.7 and C_A^o = [An]/03).

Fluorescence Intensity Calculation. The emission decay of unquenched phenanthrene in these systems is exponential with a lifetime of τ_D = 48.8 ns. In the presence of anthracene, the decay profiles deviate from a single exponential. The rate $w(r)$ of direct nonradiative energy transfer between a donor and an acceptor separated by a distance r was calculated by Förster[22]

$$w(r) = \frac{3}{2}\frac{\kappa^2}{\tau_D}\left(\frac{R_o}{r}\right)^6 \qquad (5)$$

where R_o is the Förster radius (R_o = 2.68 nm) and $^3/_2\kappa^2$ is a geometric orientation factor equal to unity for the case of rapidly reorienting chromophores ($^3/_2\kappa^2 = 1$). The form of the donor fluorescence intensity $I_D(t)$ for identical donors in the presence of acceptors was calculated by Klafter et al.[18] (eq 6).

$$I_D(t) = \exp(-t/\tau) \int C_D(r) \exp[-\varphi(r, t)]\, dr$$

$$\varphi(r, t) = \int C_A(r' - r)\{1 - \exp[-w(r')t]\}\, dr' \qquad (6)$$

The general form of $I_D(t)$ for the DET between donors and acceptors distributed in planar and spherical geometries was formulated by Yekta et al.[19,20] Here we use the equation developed by Yekta et al. for the spherical geometry to model the fluorescence intensity decay in our IPN system.

$$I_D(t) = \exp(-t/\tau) \int C_D(R) \exp[-g(R, t)]R^2\, dR$$

$$g(R, t) = 4\pi \int_\infty^0 \langle C_A(r, R)\rangle \{1 - \exp[-tw(r)]\}r^2\, dr$$

$$\langle C_A(r, R)\rangle = \frac{N_A}{2rR}\int_{r+R}^{|r-R|} r' C_A(r')\, dr' \qquad (7)$$

The topology of the IPNs as seen in the TEM image is complicated (Figure 6). The size and shape of the microphases are polydisperse. The acrylate appears to form domains with a mean size of ca. 20 nm surrounded by a urethane matrix. Furthermore, some parts of the TEM image appear to exhibit bicontinuous morphology. The presence of bicontinuous domain structures makes the analysis of the energy transfer data more difficult than that for the relatively simple model we employ here. However, it should be noted that morphology determination by TEM is obscured by the resolution of the technique. The TEM image is taken on an IPN film section ca. 100 nm thick, stained selectively with RuO_4. The observed image is therefore the superposition in two dimensions of many domains, and it may be this which gives the illusion of the bicontinuity. Although the actual structure of the IPN may not be as complicated as shown in the TEM images, our calculation of energy transfer is made difficult by the polydispersity in the size and shape of the domains. It is for this reason that we resort to a simple model of the morphology to gain insights into the domain structure. We model the morphology of these IPNs in terms of individual spherical acrylate domains of 20 nm diameter, surrounded by a shell of urethane, where the shell size is limited by the material balance ($^{30}/_{70}$ wt/wt, acrylate/urethane). We use the H−T profiles to describe the spatial dependence of anthracene−acrylate $C_A(r)$ and phenanthrene−

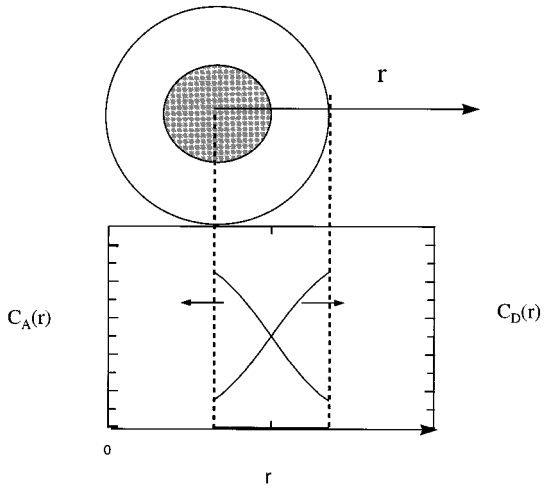

Figure 13. Representation of Helfand−Tagami profiles for a model in which spherical domains of an acceptor-labeled acrylate rich phase is dispersed in a donor-labeled urethane matrix. Here, $C_A(r)$ represents the acceptor group profile; and $C_D(r)$ the donor profile. The shaded region represents the domain in which the anthracene-labeled acrylate is the major component.

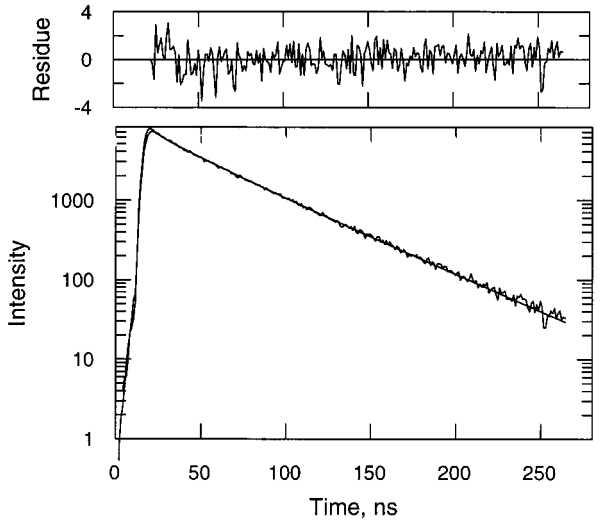

Figure 14. Experimental fluorescence decay of sample IPN3−U (noisy trace) fitted with a model $I_D(t)$ profile calculated from eq 6 (convoluted with the lamp profile). The weighted residual of the fit is also presented (top). The input parameters are $\delta = 7$ nm, [An] = 7.45 mM, $R_s = 10$ nm, and $R_o = 2.68$ nm.

urethane $C_D(r)$ concentrations in this spherical geometry (Figure 13 and eq 4a,b).

Methodology: Simulation and Fluorescence Decay Analysis. A given theoretical intensity decay curve $I_D(t)$ is calculated numerically according to eq 7 by assuming a sphere of radius $R_s = 10$ nm, introducing the known concentrations of phenanthrene and anthracene, the Förster radius ($R_o = 2.68$ nm), and an estimated interface thickness δ. The calculated intensity $I_D(t)$ is then convoluted with an experimental lamp profile[16] [Lamp(t')] using eq 8. Subsequently, the experimental decay is fitted to the calculated $I_D(t)$ to recover the intensity at time $t = 0$ (I_o) and to calculate the least-squares χ^2 value, the weighted residuals, and the autocorrelation of the residuals (Figure 14). Various δ values ranging from 0 to 15 nm were selected, and model decay traces $I_D(t)$ were calculated for each and then compared to the experimental decays. The χ^2–

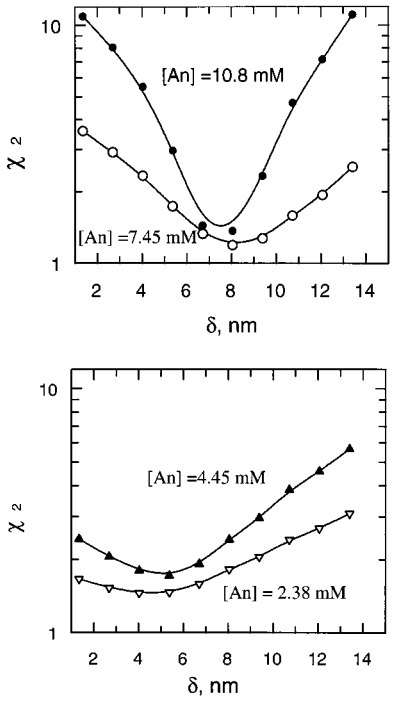

Figure 15. χ^2 surfaces from fits of experimental decays to the calculated decays as a function of the assumed interface thickness δ for various concentrations of anthracene in the acrylate phase.

surfaces resulting from these fits are plotted versus the assumed δ in Figure 15. These plots exhibit a sharp minimum at $\delta = 7-8$ nm for [An] = 10.8 mM and a broader minimum at similar δ values for lower concentrations of acceptor. In terms of the model, this establishes an apparent interface thickness of 70−80 Å.

$$I_D(t) = I_o \int I_D(t - t')\mathrm{Lamp}(t')\,dt' \qquad (8)$$

The recovered δ values depend on the input parameters such as the sphere radius R_s, the Förster radius, and the type of morphology used for the simulation. Any error in these parameters induces errors in the determination of δ. The acrylate domain sphere radius R_s used in the calculation was estimated rather roughly from TEM images of the samples and corresponds to an average domain size. The domain sizes were measured in TEM by staining the urethane matrix with RuO_4. The staining process might lead to an error of the R_s determination. To estimate the error in δ, decays were simulated by inputting a smaller sphere radius ($R_s = 7.5$ nm), and the calculated interface thickness δ was found to be shifted to a lower value ($\delta = 5$ nm).

In the simulations, we limit DET to occur within a single sphere with the donor in the outer shell and the acceptor in the interior. We neglect DET between adjacent spheres. We estimate on the basis of upon distance considerations (cf. eq 5) that the contribution of the anthracene in the neighboring domains to the phenanthrene quenching to be less than 5%, which is relatively low compared to other sources of error. The largest error may come from the choice of a spherical geometry instead of the exact domain shape. The choice of spheres can underestimate the total surface area of interface between the urethane and acrylate, which would lead to an overestimation of δ. All of these types of errors lead to an overestimate of the calculated interfacial thickness δ ($\delta = 7$ nm).

The interface thickness calculated in the urethane−acrylate IPNs ($\delta = 7$ nm) is comparable to the thickness in many polymer blends (for PS−PMMA, $\delta = 5$ nm),[13b,c] but unfortunately, we do not as yet have independent data on the interface thickness in polyurethane−polyacrylate blends. We also note that the IPN with a high degree of cross-linking density was found to exhibit the same extent of mixing as that in the semi-IPNs, which more closely resemble simple polymer blends. Therefore, the extent of interfacial mixing in the IPNs might not be very different from that of polymer blends. The cross-linking of the urethane might lead to formation of small domains due to spatial restrictions, but the extent of interfacial mixing might be controlled by polymer immiscibility.

In the model described here, neither component forms a pure phase because the interfacial thickness recovered ($\delta = 7$ nm) is on the order of the size of the domains. We estimate that even in the center of the acrylate domain, there is still ca. 5% urethane. These results are consistent with results presented in our previous work on similar samples.[9] The composition and processing history of the IPNs examined here are the same as those examined by Yang et al.,[9] but the locus of the dyes are different. We would expect that both types of labeling patterns should yield consistent descriptions of the IPN morphology. In the previous work, the phenanthrene and anthracene dyes were both incorporated into the urethane phase. Here, the mixing of the acrylate and urethane polymers dilutes the dyes relative to a pure polyurethane phase. The results were analyzed in terms of a model with two types of domains, without taking into consideration the spatial restriction of the domains. From this very simple point of view, the urethane-rich phase was calculated to be made up of 22 vol % acrylate and 78 vol % urethane. The interface thickness in the H−T profiles ($\delta = 7$ nm) found in the present analysis is comparable to the domain size ($R_s = 10$ nm) and to the shell size (5 nm). Thus within such domains, no phase is truly pure; the urethane-rich phase contains some of the acrylate and vice versa. Our model would accommodate pure phases only if the domain size were large enough compared with the interfacial thickness.

Acknowledgment. The authors thank 3M, 3M Canada, Inc., and NSERC Canada for their support of this research.

References and Notes

(1) Sperling, L. H.; Mishra, V. In *IPNs Around the World*; Kim, S. C., Sperling, L. H., Ed.; Wiley: New York, 1997.
(2) Sperling, L. H. *Interpenetrating Polymer Networks and Related Materials*; Plenum Press: New York, 1981.
(3) *Advances in Interpenetrating Polymer Networks*; Klempner, D., Frisch, K. C., Eds.; Technomic Publishing Co.: Lancaster, PA, 1989; Vols, I−III.
(4) Roesler, R. R. *Mod. Paint Coat.* **1986**, April, 46.
(5) Keipert, S. J.; Kinzer, K. E.; Brown, A. M. *Met. Finish.* **1994**, March, 53.
(6) De Gennes, P. G. *J. Phys., Lett.* **1979**, *40*, L-69.
(7) Skinner, E.; Emeott, M.; Jevne, A. U.S. Patent 4,342,793, 1982.
(8) Fox, R. B.; Bitner, J. L.; Hinkley, J. A.; Carter, W. *Polym. Eng. Sci.* **1985**, *25*, 157.
(9) Yang, J.; Winnik, M. A.; Ylitalo, D.; DeVoe, R. J. *Macromolecules* (a) **1996**, *29*, 7047; (b) 7055.
(10) Yang, J.; Winnik, M. A. *Chem. Phys. Lett.* **1995**, *238*, 25.
(11) Ring, W.; Mita, I.; Jenkins, A. D.; Bikales, N. M. *Pure Appl. Chem.* **1985**, *57*, 1427.
(12) Helfand, E.; Tagami, Y. *J. Chem. Phys.* **1972**, *56*, 3592.
(13) (a) Feng, J.; Yekta, A.; Winnik, M. A. *Chem. Phys. Lett.* **1996**, *260*, 296−301. (b) Ni, S.; Zhang, P.; Wang, Y.; Winnik, M. A. *Macromolecules* **1994**, *27*, 5742. (c) Russel, T. P.; Menelle, A.; Hamilton, W. A.; Smith, G. S.; Satija, S. K.; Majkrzak, C. F. *Macromolecules* **1991**, *24*, 5721.
(14) Miles, I. S. In *Multicomponent Polymer Systems*; Miles, I. S., Rostami, S., Ed.; Harlow: Burnt Mill 1992.
(15) (a) Brulet, A.; Doud, M.; Zhou, P.; Frisch, H. L. *J. Phys. II* **1993**, *3*, 1161. (b) Abetz, V.; Meyer, G. C.; Mathis, A.; Picot, C.; Widmaier, J. M. In *IPNs Around the World*; Kim, S. C., Sperling, L. H., Ed.; Wiley: New York, 1997. (c) Parizel, N.; Meyer, G.; Weill, G. *Polymer* **1995**, *36*, 2323.
(16) O'Connor, D. V.; Philips, D. *Time-Correlated Single Photon Counting*; Academic Press: London, 1984.
(17) Birks, J. B. *Photophysics of Aromatic Molecules*; Wiley-Interscience: New York, 1970.
(18) Klafter, J., Blumen, A., Drake, J. M., Ed. *Molecular Dynamics in Restricted Geometries*; Wiley: New York, 1989.
(19) Yekta, A.; Duhamel, J.; Winnik, M. A. *Chem. Phys. Lett.* **1995**, *235*, 119.
(20) Yekta, A.; Winnik, M. A.; Farinha, J. P. S.; Martinho, J. M. G. *J. Phys. Chem. A.* **1997**, *101*, 1787.
(21) Evans, D. F.; Upton, M. W. *J. Chem. Soc., Dalton Trans.* **1985**, 1141−1145.
(22) Förster, T. *Discuss. Faraday Soc.* **1959**, *27*, 7.
(23) Perrin, F. *Compt. Rend.* **1924**, 178, 1978.
(24) Yang, J.; Winnik, M. A. *Can. J. Chem.* **1995**, *73*, 1823.
(25) We have found that somewhat better quality data can be obtained by measuring phenanthrene fluorescence decays at 350−355 nm.

MA9815612